Sedimentology (1999) **46**, 791–805

Sediment resuspension and transport in Lake Michigan during the unstratified period

NATHAN HAWLEY* and CHANG-HEE LEE†,[1]
**Great Lakes Environmental Research Laboratory (E-mail: hawley@glerl.noaa.gov), and †Cooperative Institute for Limnology and Ecosystems Research, 2205 Commonwealth Blvd, Ann Arbor, MI 48105, USA*

ABSTRACT

Instrumented moorings were deployed during the winter of 1994–95 at three depths (28, 58 and 101 m) in southern Lake Michigan. Storms during the observation period were not unusually severe, so the processes observed are typical of those that occur during an average winter. Time series observations of water temperature, beam attenuation coefficient (a measure of water transparency) and current velocity show that local resuspension of bottom sediment occurred frequently after the breakdown of the thermocline. Resuspension was most frequent close to the shore but was also observed at the 58 m station. Local resuspension did not occur at the 101 m station, but advection to the site of material resuspended at shallower sites was observed. These observations do not support the hypothesis proposed by previous investigators that local resuspension at depths of 100 m or greater occurs during the unstratified period. It is more likely that fine-grained material resuspended by storm action in intermediate water depths (≈ 30–60 m) is transported into the deeper parts of the lake by the general lake circulation.

Keywords Bottom currents, Lake Michigan, limnology, resuspension, sediment transport, surface waves.

INTRODUCTION

The transport of fine-grained material in the Lawrentian Great Lakes is poorly understood. Most of this material is introduced into the lakes by either tributaries or shoreline erosion (Rea *et al.*, 1981; Colman & Foster, 1994) and then transported to offshore depositional areas (Edgington & Robbins, 1990), but exactly how and when this transport occurs is not well known. Recent model studies of the cycling of various chemicals in the Great Lakes conclude that, during the unstratified period (approximately November through May), bottom material is resuspended in the deeper parts of the lakes and distributed relatively evenly throughout the water column (Oliver & Charlton, 1984; Oliver *et al.*, 1989; Baker *et al.*, 1991; Robbins & Eadie, 1991). The data for these models have come primarily from sediment trap studies, but while sediment traps can provide important information on the variations in the material suspended in the water column, they do not by themselves provide any information on the processes responsible for these variations. Although these model studies recognized the importance of suspended sediment in the cycling process, none of them included measurements of the physical processes involved in resuspending and transporting suspended material.

Time series observations of both current (and/or wave) activity and suspended sediment concentration are necessary to determine the physical processes responsible for the resuspension and transport of suspended material, but only a small number of such studies have been under-

[1]Present address: Division of Environmental Policy, Korean Environmental Institute, Daesong Building, 1049-1, Sadong Dong, Dongjak-Gu, Seoul 156-090, Republic of Korea

© 1999 International Association of Sedimentologists

taken in the Great Lakes. To date, the only such observations made during the unstratified period are those of Hawley & Lesht (1995) from Lake Michigan in the spring of 1984 and 1987. They observed no instances of bottom resuspension at depths of 60–70 m, even though relatively large storms (peak wind speeds of 14–16 m s^{-1}) occurred during both deployments. However, the maximum near-bottom current speeds were only about 0·10 m s^{-1} and were not apparently large enough to resuspend bottom material. Hawley & Lesht (1995) concluded that bottom resuspension occurred infrequently at depths greater than wave base (about 30 m), and that lateral advection of material suspended in shallower water was probably responsible for most of the variations in suspended sediment concentration observed in the deeper parts of the lake. In another study, Hawley *et al.* (1996) combined current velocity measurements with chemical analyses of material collected by a sequencing sediment trap during two deployments at a station in Lake Ontario in 55 m of water. The first deployment covered the period of the breakdown of the thermocline (mid-October to mid-December), and the second occurred during the time of the formation of the thermal bar (mid-April to the end of June). No evidence of resuspension was found during the April–June deployment, but several episodes of local bottom resuspension probably occurred during the October–December deployment. Based on the chemistry of the trap material, they also concluded that significant alongshore transport occurred at least once during November. Both of these studies were limited by the fact that observations were made in only one location at any given time, so it was not possible to determine the role of offshore transport.

This study reports results obtained during the unstratified period from a series of three instrument moorings located on a cross-shelf transect in southern Lake Michigan. The observations from the three stations show the effects of storms on sediment resuspension and transport in the lake during the unstratified period. Two specific hypotheses are addressed: (1) storm action causes sediment resuspension in the deeper parts of the lakes (below wave base); and (2) the general lake circulation transports material resuspended in the nearshore zone to offshore areas. Lee & Hawley (1998) described results from the same sites during August–October 1995, but found little evidence of sediment resuspension during that period.

STUDY SITE AND METHODS

Lake Michigan is one of the Lawrentian Great Lakes located near the middle of North America (Fig. 1). Boyce *et al.* (1989) have reviewed the seasonal thermal cycle of these lakes and described the various physical processes that occur. Circulation in the lakes is driven by the wind, but the effects of the earth's rotation are also important. The effects of storm action on sediment movement are most pronounced during the unstratified period, when the higher wind speeds

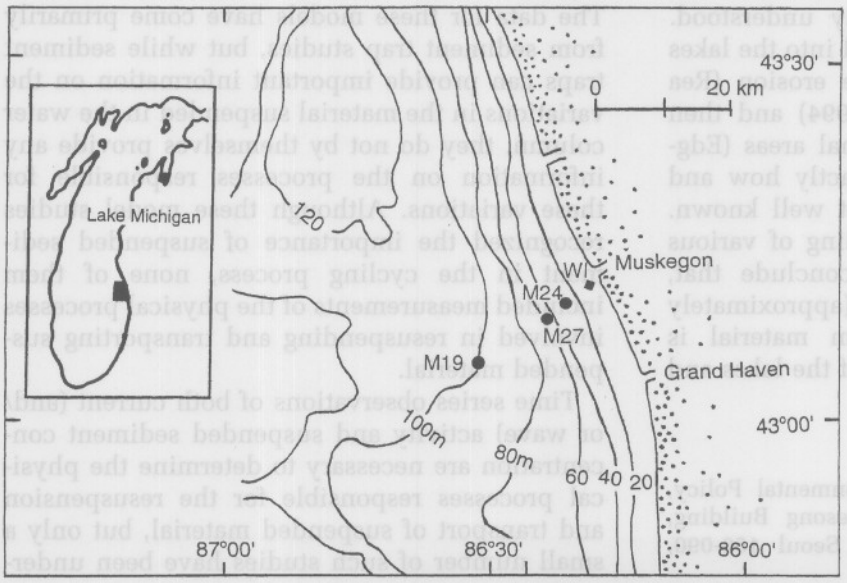

Fig. 1. Location of the moorings and the water intake station (WI).

and the absence of a thermocline allow the effects of wind action to penetrate deeper into the water column. In shallow water, the entire water mass moves in the direction of the wind, while a return flow occurs in the deeper parts of the lake. This causes a counterclockwise-rotating, two-gyre circulation pattern, which persists after the wind forcing ceases. Regions of cross-shore transport migrate along the coast as the gyres rotate, and the rotation may also explain the tendency of coastal currents to reverse direction several days after a strong wind event. These rotary motions, which are called topographic or vorticity waves, have been described in Lake Michigan by Saylor *et al.* (1980).

As part of the Lake Michigan Mass Balance Study conducted by the US Environmental Protection Agency, instrument moorings were deployed at three sites in south-eastern Lake Michigan on 31 October 1994 and retrieved in late May 1995. The sites were located in water depths of 28 m, 58 m and 101 m on a transect running approximately south-west from Muskegon, Michigan (Fig. 1). The shallowest station (M24) was at a depth at which direct surface wave action was likely to reach the bottom, and the deep station (M19) was located at a point where a set of current meters and sediment traps had been deployed by other investigators. The middle station (M27) was located at a depth about halfway between the other two. Additional observations of water transparency and temperature were obtained from the municipal water intake for the city of Muskegon, Michigan (station WI in Fig. 1).

Water depth along the transect increases gradually to about 30 m, then more rapidly to about 80 m, after which it increases gradually along the lake floor to a maximum depth of about 165 m in the southern basin. Bottom samples at the stations were collected and analysed by Lee & Hawley (1998), who found that the bottom was non-cohesive at the water intake and at M24, and cohesive at M27 and M19. Observations made with a remotely operated vehicle showed that the bed was rippled at the water intake site and flat at the other stations. The mean grain size for each station is given in Table 1; the sand-sized fraction

Table 1. Deployment data.

Station	Water intake	M24	M27	M19
Deployed	–	31 Oct 1994	31 Oct 1994	31 Oct 1994
Retrieved	–	25 May 1995	25 May 1995	24 May 1995
Latitude	43°12·30′ N	43°13·75′ N	43°09·50′ N	43°02·93′ N
Longitude	86°20·83′ W	86°25·46′ W	86°25·87′ W	86°38·57′ W
Water depth (m)	13	28	58	101
Electromagnetic current velocity measurements				
Height (mab)	–	0·5	35	35
Sampling rate (Hz)	–	2	1	1
Sampling period	–	1 min/hour	1 min/hour	1 min/hour
Vector averaging current velocity measurements				
Height (mab)	–	–	–	5, 75
Sampling rate	–	–	–	Continuous
Sampling period	–	–	–	15-min average
Temperature measurements				
Height (mab)	3	0·9, 7, 17	35	0·9, 7, 17, 35, 65
Sampling rate	Hourly	1 Hz	1 Hz	1 Hz
Sampling period	Single measurement	1 min/hour	1 min/hour	1 min/hour
Transparency measurements				
Height (mab)	3	0·9,7,17	35	0·9,7,17,35,65
Sampling rate	Two-hourly	1 Hz	1 Hz	1 Hz
Sampling period	Single measurement	1 min/hour	1 min/hour	1 min/hour
Bottom sediment size analyses				
Percentage sand	100	94	55	40
Percentage silt	0	5	42	44
Percentage clay	0	1	4	16
Mean diameter (mm)	0·26	0·24	0·16	0·14

at all stations was predominantly fine (0·125–0·25 mm) and medium (0·25–0·5 mm) sand. The mineralogy of the lake bed is primarily quartz, with smaller amounts of feldspar, carbonates and clay minerals (Rea *et al.*, 1981).

Time series measurements of temperature, current velocity and water transparency were made at the elevations given in Table 1. Marsh-McBirney 585 and Interocean S4 electromagnetic current meters were used to measure the current velocities. Calibrations made in a towing tank before deployment show that the current meters have a resolution of 0·005 m s^{-1} and an accuracy of 0·01 m s^{-1}. As two of the electromagnetic current meters at M19 failed, data from EG & G vector-averaging current meters (VACM) deployed at the station by other investigators were used instead. The VACMs have a lower threshold of 0·02 m s^{-1} and an accuracy of 0·01 m s^{-1}.

Temperature measurements were made using Yellow Springs thermistors accurate to 0·2 °C. Water transparency measurements were made using Sea Tech transmissometers (0·25 m pathlength) and Sea Tech light-scattering sensors (LSS). The transmissometer and light-scattering sensor readings were recorded to the nearest 0·001 volt over a nominal 5-volt scale. Although the readings of both the transmissometers and the LSS respond to changes in the suspended sediment concentration, each LSS responded differently to these changes when compared with the beam attenuation coefficient (BAC; which is independent of the instrument used) calculated from the transmissometer readings. Bottom material from M27 was used to perform a five-point calibration between the voltage reading for each LSS and the BAC measured by a transmissometer. These data were used to construct a separate correction equation for each of the LSS sensors. The correction equations varied significantly from sensor to sensor, but the r^2 values were all greater than 0·99. Hawley & Zyren (1990) have shown that there is a linear relationship between BAC and the concentration of suspended particulate material (SPM) in Lake Michigan so, in this paper, BAC is used as a surrogate for SPM. All instruments (except for the VACMs, which recorded a continuous 15-min average) were sampled at 1 Hz for 1 min every 1 h; the averaged values and their standard deviations were then recorded.

Temperature at the water intake was measured hourly but, because turbidity was measured every other hour, an averaged value between each two measurements was used to obtain an hourly record. The turbidity readings were reported in nephelometric turbidity units (NTUs). These were converted to BAC by determining the BAC at 5 NTU levels and constructing a correction equation. These measurements were made using the same standard turbidity solution used to calibrate the water intake's turbidity meter. Because a time lag of up to 6 h could exist between the time the water entered the intake and the time that the measurements were made at the station on shore, the intake records were shifted 6 h before plotting. However, as the time lag was not constant, the intake data are not always simultaneous with the other measurements.

Vertical profiles of water temperature and transparency were made using a Sea Bird SBE 19 profiler equipped with a Sea Tech transmissometer (0·25 m pathlength) on the deployment date, on 5 December and in late (24–25) January. The profiles made in January show that, by this time, all of the LSS had become at least slightly fouled by the growth of biological material on the sensors. The fouling causes an increase in both the BAC and the variation in the BAC (as a result of the logarithmic transformation involved in converting the voltage reading to BAC). There is no good way to correct the data for this fouling and, as these measurements are not used quantitatively, no corrections were made. There were also several other instrument problems. The tripod at station 27 failed completely; the current meter at M24 stopped in mid-February; and there are short gaps in several of the other records. As noted above, two of the current meters at M19 also failed, so data from the VACM current meters located 5 m and 75 m above the bottom (mab) at this station were used instead.

As no wave observations were made during the deployment, the GLERL wave model (Schwab *et al.*, 1981) and weather observations from around the lake were used to calculate the significant wave height and peak energy wave period. A comparison of the model output with observations of the wave parameters made during the autumn of 1995 shows that, although the wave model calculates the wave height quite well (r^2 = 0·87 for 1189 observations), it does not determine the wave period very accurately (r^2 = 0·47). In general, the wave model calculates periods longer than those observed, particularly for periods longer than 4 s. A linear correction has been applied to the model periods longer than 4 s (r^2 = 0·66 based on 419 observations). Wind measurements collected as part of the mass balance study are reported from a weather station

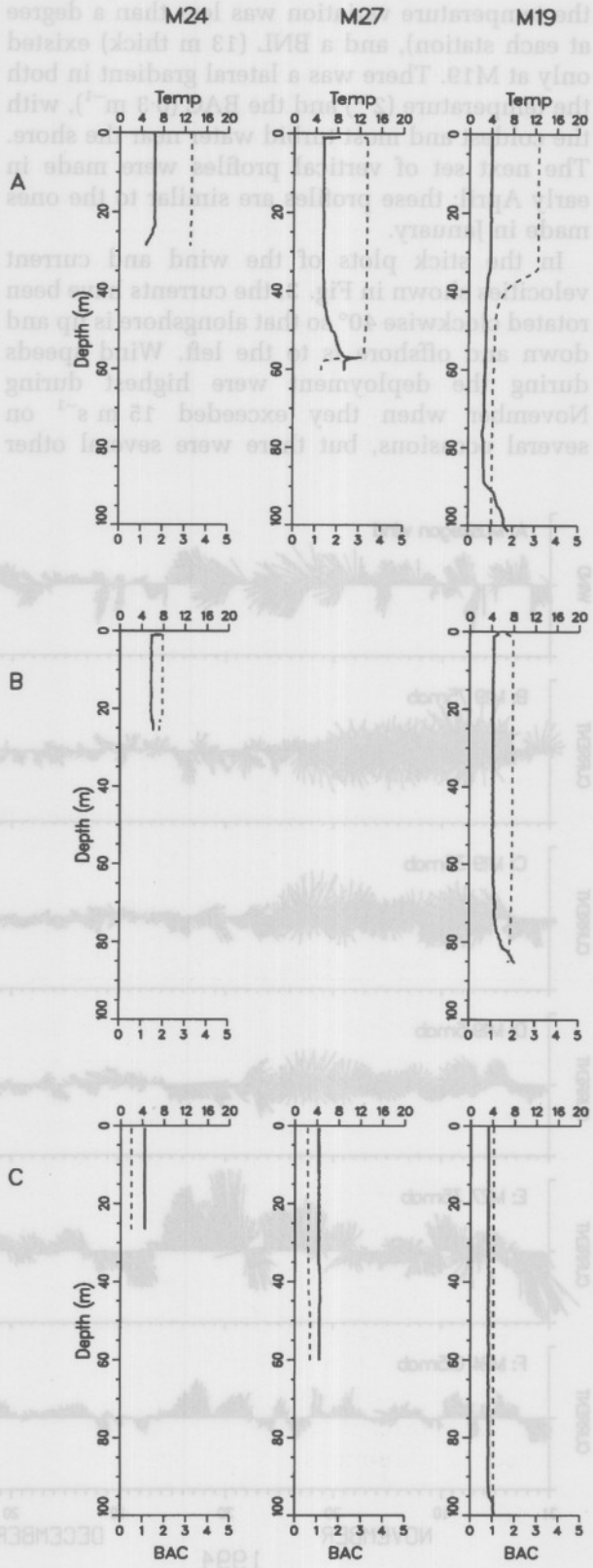

Fig. 2. Vertical profiles made at the three mooring stations. The solid line is the BAC (beam attenuation coefficient) and the dashed line is the temperature. (A) Profiles made on the deployment date, 31 October 1994. (B) Profiles made on 5 December. No profile was made at M27, and only a partial profile was made at M19. (C) Profiles made on 24 January (M19 and M27) and 25 January (M24).

located at the field station of the Great Lakes Environmental Research Laboratory, which is located at the mouth of the Muskegon River (Fig. 1).

Particle flux measurements were made at M19 with sequencing sediment traps 0·20 m in diameter and an aspect ratio (trap height divided by trap diameter) of 8:1. The traps have a series of collection bottles mounted in a carousel at the bottom of the trap that can be programmed to advance at user-specified intervals. These traps are described in more detail by Eadie (1997), who determined a measurement error of 14%.

RESULTS

As the fouling of several of the optical sensors at both M27 and M19 became much worse after the end of January (the LSS at M24 became completely fouled in December) and as the current meter at M24 stopped working in mid-February, the analysis is restricted to the period from 31 October to 18 February. Data from the vertical profiles on the deployment date (Fig. 2) show that, although the lake was still stratified, the breakdown of the thermocline had begun and the depth of the surface mixed layer exceeded 30 m. The benthic nepheloid layer (BNL) is usually defined as a region extending upwards from the bottom in which the BAC is greater than the minimum value of the BAC in the middle part of the water column. The top of the BNL is then defined as the lowest elevation above the bottom at which the BAC is at a minimum. On 31 October, there was no BNL at M24 where the water was isothermal (in fact, the water is clearer near the bottom), but a BNL was present at both M27 (21 m thick) and at M19 (32 m thick). The profiles made at M24 and M19 (upper 85 m only) on 5 December show that the water was almost isothermal at both stations (the change in temperature was less than a degree at both M24 and M19) and that there was a BNL 7 m thick at M24 and 40 m thick at M19. In late January, the water was almost isothermal at all of the stations (again

the temperature variation was less than a degree at each station), and a BNL (13 m thick) existed only at M19. There was a lateral gradient in both the temperature (2 °) and the BAC (0·3 m^{-1}), with the coldest and most turbid water near the shore. The next set of vertical profiles were made in early April; these profiles are similar to the ones made in January.

In the stick plots of the wind and current velocities shown in Fig. 3, the currents have been rotated clockwise 40° so that alongshore is up and down and offshore is to the left. Wind speeds during the deployment were highest during November when they exceeded 15 m s^{-1} on several occasions, but there were several other storms during the rest of the deployment. However, none of these storms can be considered extraordinary; a survey of 32 years of wind records shows that the most severe storms during the deployment have a recurrence interval of about 1 year (Transport Canada, 1991). The rotary motion seen in the early parts of the velocity records at M27 (before 18 November) and M19 (before 1 December) are caused by near-inertial internal waves. These waves are a ubiquitous feature of the offshore lake circulation during the stratified period (Boyce *et al.*, 1989), so their absence after November is a strong indication that the thermocline had broken down. Currents at M24 and M27 are oriented primarily

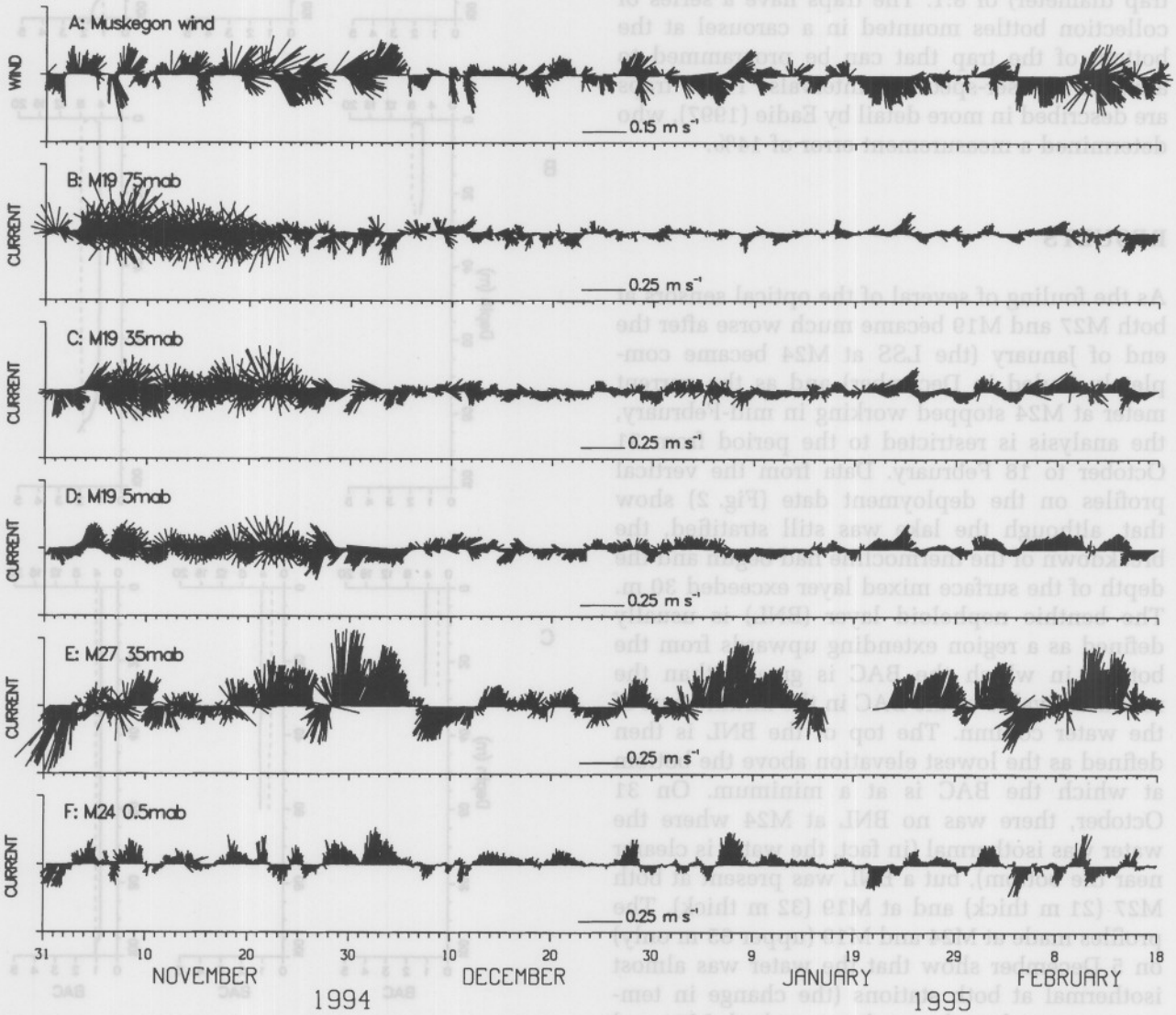

Fig. 3. Stick plots of the wind and current velocities. All data are rotated 40° so that alongshore is top–bottom and offshore is to the left. Gaps in the records indicate that no data are available. (A) Wind at Muskegon dock. (B) Currents 75 mab at M19. (C) Currents 35 mab at M19. (D) Currents 5 mab at M19. (E) Currents 35 mab at M27. (F) Currents 0·5 mab at M24.

alongshore as a result of topographic steering and are frequently in the opposite direction to the wind. The lower speeds at M24 are partly due to the lower elevation of the current meter above the bottom (0·5 mab at M24 and 35 mab at M27). Water movement at both stations usually has an offshore component when the current is to the south and an onshore component when the current is to the north. After the breakdown of the thermocline at M19, the current speeds are much lower than those at M27, are fairly consistent from top to bottom and have a much greater cross-shore component than the currents at the inshore stations.

The time series observations from the water intake station, M24, and M27 are shown in Fig. 4. The temperature records at M24 show that the water was isothermal after about 10 November and that it then cooled throughout the rest of the deployment. The temperature record at M27 is similar to those at M24 so, by mid-November, the water was probably also isothermal at this station. Upwelling events beginning on 2 and 6 November contributed to the breakdown of the thermocline

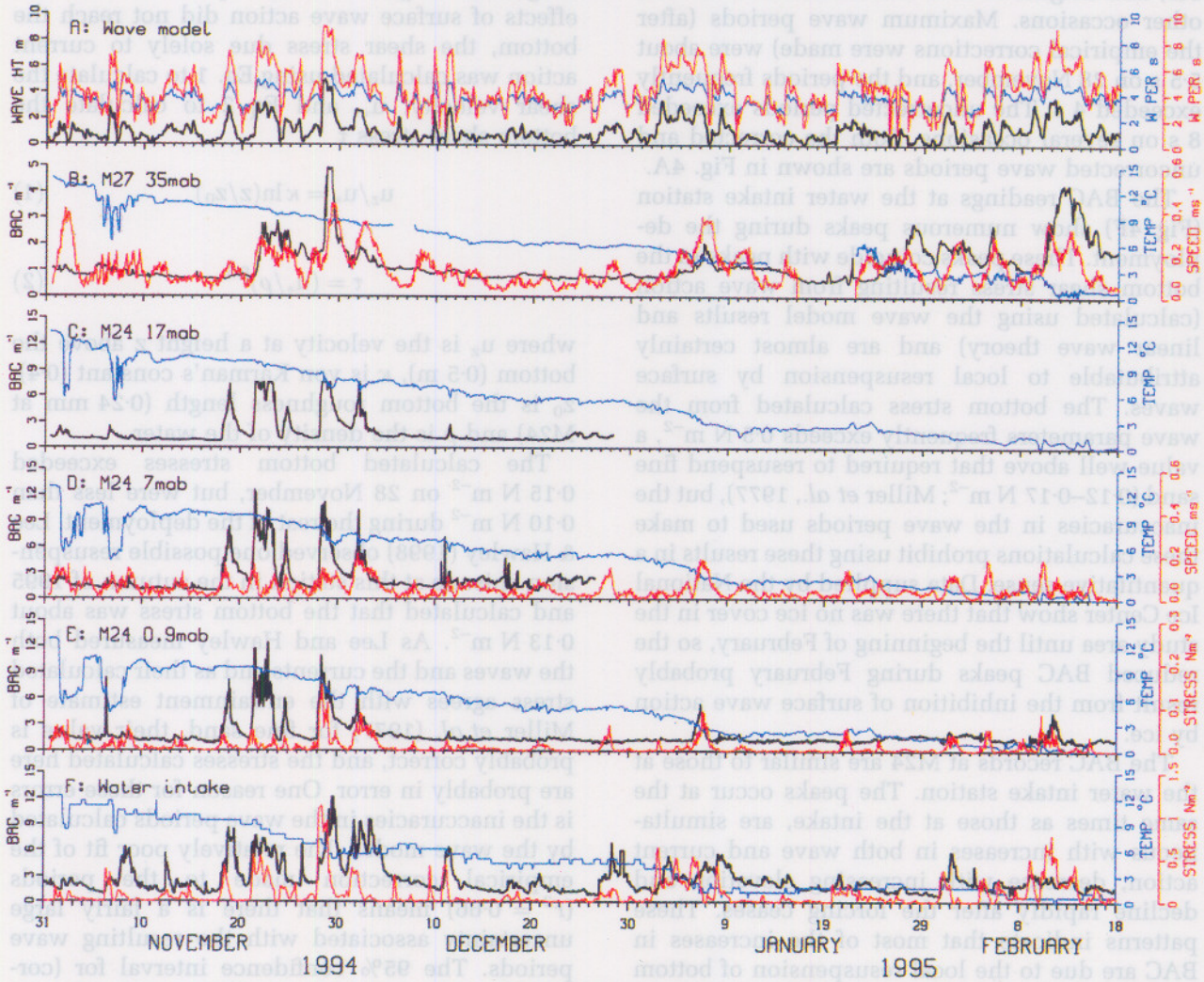

Fig. 4. Time series data from the intake station, M24, and M27. Gaps in the data indicate that no data are available. Except in Fig. 4A, the black line is the BAC (m^{-1}), the red line is either the shear stress ($N\ m^{-2}$) or current speed ($m\ s^{-1}$) and the blue line is the temperature (°C). (A) Wave height in m (black), and wave period in s. The blue line is the wave period after the corrections have been applied, and the red line is the uncorrected wave period. (B) BAC, current speed and temperature 35 mab at M27. Note that the BAC scale is different in this plot. (C) BAC and temperature 17 mab at M24. The LSS became severely fouled after 28 December. (D) BAC and temperature 7 mab and current speed 0·5 mab at M24. The LSS became severely fouled after 26 December. (E) BAC and temperature 0·9 mab and bottom shear stress resulting from combined wave and current action at M24. (F) BAC, temperature and bottom shear stress resulting from wave action at the water intake station.

at these stations. The upwelling on 6 November also produced a peak in the BAC record at both the water intake and M24; changes in BAC during similar events are discussed by Lee & Hawley (1998). The short-period oscillations at the beginning of the temperature records at both stations are caused by the internal near-inertial waves mentioned above. The presence of these waves is also evident in the current speed record at M27. Current speeds at M27 are higher than at M24, but both sets of observations show the same general pattern of increases and decreases. Calculated wave heights of over 5 m occurred on 28 November, and heights of over 3 m occurred on several other occasions. Maximum wave periods (after the empirical corrections were made) were about 5·5 s on 28 November, and the periods frequently exceeded 4 s. The uncorrected periods exceeded 8 s on several occasions. Both the corrected and uncorrected wave periods are shown in Fig. 4A.

The BAC readings at the water intake station (Fig. 4F) show numerous peaks during the deployment. These peaks coincide with peaks in the bottom shear stress resulting from wave action (calculated using the wave model results and linear wave theory) and are almost certainly attributable to local resuspension by surface waves. The bottom stress calculated from the wave parameters frequently exceeds 0·5 N m^{-2}, a value well above that required to resuspend fine sand (0·12–0·17 N m^{-2}; Miller *et al.*, 1977), but the inaccuracies in the wave periods used to make these calculations prohibit using these results in a quantitative sense. Data supplied by the National Ice Center show that there was no ice cover in the study area until the beginning of February, so the reduced BAC peaks during February probably result from the inhibition of surface wave action by ice.

The BAC records at M24 are similar to those at the water intake station. The peaks occur at the same times as those at the intake, are simultaneous with increases in both wave and current action, decrease with increasing elevation and decline rapidly after the forcing ceases. These patterns indicate that most of the increases in BAC are due to the local resuspension of bottom material. Some of the BAC peaks seen at the water intake are not seen at M24 (those on 11 and 28 December, for instance); this is probably because of the greater water depth at M24, which would result in a decreased bottom shear stress resulting from wave action. The light-scattering sensors at the upper two levels at M24 became badly fouled in late December (these data are not shown), but the bottom transmissometer shows peaks in BAC on 6 January and 10 February.

Because of the greater water depth at M24, the bottom stress resulting from wave action is much less than at the water intake, and the bottom stress caused by current action may be important. Wave parameters from the wave model and the current meter data from M24 were used as input to the Kim *et al.* (1997) model to calculate the bottom shear stress resulting from combined waves and currents at this station (Fig. 4E; as there were no observations of bedforms at this site, the mean grain size was used as the bottom roughness length). For time periods when the effects of surface wave action did not reach the bottom, the shear stress due solely to current action was calculated using Eq. 1 to calculate the shear velocity, u_*, and Eq. 2 to calculate the bottom shear stress τ

$$u_z/u_* = \kappa \ln(z/z_0) \quad (1)$$

$$\tau = (u_*/\rho)^{0.5} \quad (2)$$

where u_z is the velocity at a height z above the bottom (0·5 m), κ is von Karman's constant (0·4), z_0 is the bottom roughness length (0·24 mm at M24) and ρ is the density of the water.

The calculated bottom stresses exceeded 0·15 N m^{-2} on 28 November, but were less than 0·10 N m^{-2} during the rest of the deployment. Lee & Hawley (1998) observed one possible resuspension episode at this station in the autumn of 1995 and calculated that the bottom stress was about 0·13 N m^{-2}. As Lee and Hawley measured both the waves and the currents and as their calculated stress agrees with the entrainment estimate of Miller *et al.* (1977) for fine sand, their value is probably correct, and the stresses calculated here are probably in error. One reason for these errors is the inaccuracies in the wave periods calculated by the wave model. The relatively poor fit of the empirical correction made to the periods ($r^2 = 0{\cdot}66$) means that there is a fairly large uncertainty associated with the resulting wave periods. The 95% confidence interval for (corrected) wave periods of 4·7–5·5 s (the values calculated during the resuspension episodes) is about 0·75 s. However, even if the upper bound of this interval is used for the wave periods, the periods are still mostly less than 6 s, and the resulting stresses are still below 0·10 N m^{-2}.

Lee & Hawley (1998) calculated a bottom stress of 0·13 N m^{-2} when the wave height was 3·2 m

and wave period was 6·0 s but, when the waves were slightly smaller (heights of 2·5–2·9 m and periods of 5·2–5·6 s), the stresses were much lower (0·10 N m^{-2} or less). Tests with the Kim *et al.* (1997) model show that, for a water depth of 28 m, the bottom shear stress is extremely sensitive to small changes in the wave parameters for values of the wave height between 3 and 4 m and values of the wave period around 6 s. For instance, for the same current speed and direction, a wave with a height of 3·2 m and a period of 6·0 s produces a bottom shear stress of 0·14 N m^{-2}, while a wave with the same height and a period of 6·2 s produces a shear stress of 1·2 N m^{-2}. The BAC observations clearly show that bottom resuspension did occur and, although it is likely that the bottom stress was 0·15 N m^{-2} or greater during these events, an accurate calculation of the bottom shear stress cannot be made from the available data.

BAC levels at M27 are considerably less than at M24, but there are three large peaks during the deployment (beginning on 22 and 28 November and 10 February; Fig. 4B). The increases in BAC correlate with increases in current speed but, without any near-bottom observations of either BAC or current velocity, it is difficult to determine whether local resuspension occurred. If resuspension did occur, then it must be the result of current action alone as the water depth at M27 (58 m) is too great for resuspension to be induced by surface waves. If the peaks in BAC are caused by the offshore transport of material resuspended in shallower water, then there should be a time lag between both the increase in BAC at M24 (where bottom resuspension did occur) and the increase at M27, and also some indication of offshore transport in the current velocities. On the other hand, if the increases in BAC are caused by local resuspension, then the increases in BAC should correlate with an increase in current speed regardless of the current direction.

As resuspended material is also transported laterally while it diffuses upward to 35 mab, the observations cannot distinguish between material resuspended in an area near (but not at) the site and material resuspended at the site itself. If conditions are different at other sites within this area, then the interpretation presented here could be incorrect. The actual diffusion time cannot be calculated without near-bottom observations, but Lavelle *et al.* (1984) showed that fine-grained resuspended material will reach 20 mab in about 2 h at velocities over 0·2 m s^{-1}. As the eddy viscosity far away from the bottom should be roughly constant for a given speed, the diffusion time at our site should be 3–4 h at most. Even if the alongshore velocity is 0·3 m s^{-1} (this is greater than the maximum during the deployment), the transport rate is only about 1 km h^{-1}, so the short diffusion time means that only material resuspended at sites within a few kilometres (in the alongshore direction) of the station is indistinguishable from material resuspended at the site itself. As the bottom contours in this area are shore parallel for at least 10 km to the north and south, differences in bottom sediment in the alongshore direction are probably not an important factor in explaining the observations. A similar calculation can be performed for the cross-shore transport. The maximum offshore transport in any 4 h is only about 1·2 km. The water depth at a station 1·2 km directly onshore of M27 is about 45 m, so material resuspended at this depth or greater may be indistinguishable from that resuspended at M27. As this depth is still considerably greater than wave base (30 m), as at M27, any bottom resuspension would have to be due to current action. Bottom material from the 45 m site has a size distribution and composition almost identical to that at M27, so it is unlikely that differences in either water depth or bottom sediment affect the interpretations presented here.

The BAC event that began on 10 February is clearly caused by local resuspension. The rise in BAC at M27 began about 3 h after an increase in current velocity, and there is no indication of offshore movement at either station at the beginning of the event. Although the initial rise in BAC began 3 h after the velocity reached about 0·15 m s^{-1}, it increased rapidly only after the velocity increased to about 0·3 m s^{-1} (also after about a 3 h time lag). High BAC values then persisted for several days until the current speed decreased below 0·2 m s^{-1}. The event on 22 November also resulted from local resuspension: the increase in BAC lagged behind both the initial increase in speed and the increase in BAC at M24 by about 10 h; there is no indication of offshore transport at either station; and the increase in BAC began about 2 h after the velocity reached about 0·2 m s^{-1}. The event that began on 28 November, however, is due to advection. On this occasion, the increase in BAC preceded a rapid increase in current speed, but lagged behind the increase in BAC at M24 by about 8 h. The beginning of the period of increased BAC also coincided with a change in the alongshore component of the current direction from south to north (Fig. 3E), and the currents at both stations

have an offshore component. Although the total offshore transport at both stations during the 8 h (about 1 km at M27 and about 0·5 km at M24) is less than the distance between the two stations (5 km), it seems likely that material suspended at a depth between 28 m and 58 m was transported to M27. Local resuspension may also have occurred at M27 when the current speed was high enough, but the initial increase in BAC must be the result of advected material. There are other large increases in current speed at M27 (on 1 December, 6 January and 5 February) that produced smaller increases in the BAC; these are probably also resuspension events. Because of the alongshore transport during these events and because it requires some time for resuspended material (from any site) to diffuse to 35 mab, the actual sites of erosion in all three of the major events must be several kilometres south of both M24 and M27. However, there is no reason to believe that either the currents or the bottom material at these sites differs significantly from those at M27.

Without near-bottom current measurements at M27, there is no totally satisfactory way of calculating the bottom stress during the resuspension events, but an estimate can be made based on the relationship between the near-bottom (5 mab) speeds and the 35 mab speeds measured at M19. A linear regression of the current speeds at the two elevations shows that the speed varied only slightly with elevation above the bottom during the unstratified period (after 1 January) when both speeds exceeded 0·08 m s^{-1}:

$$u_5 = 0.73^{*}u_{35} + 0.02 \qquad (3)$$

where u_5 is the current speed 5 mab, and u_{35} is the current speed 35 mab (both in m s^{-1}) at M19. Equation 3 ($r^2 = 0{\cdot}75$ based on 282 observations) and the 35 mab current speeds at M27 were used to calculate the current speed 5 mab at M27. Saylor & Miller (1988) have shown that a logarithmic layer up to 10 m thick exists in the lake during storm events, so the 5 mab data and Eqs 1 and 2 were used to calculate the bottom stress. These calculations show that when the speed 35 mab equalled 0·2 m s^{-1}, the bottom stress was about 0·04 N m^{-2}; when the 35 mab speed was 0·3 m s^{-1}, the bottom stress was about 0·09 N m^{-2}; and at 0·4 m s^{-1}, it was about 0·15 N m^{-2}. The 95% confidence intervals for the calculated shear stresses are fairly large (0·01 N m^{-2} at u_{35} equal 002 m s^{-1}, 0·02 N m^{-2} at 0·3 m s^{-1}, and 0·03 N m^{-2} at 0·4 m s^{-1}), so the peak velocities observed are probably sufficient to erode the bottom even though the mixture of sand and mud present may be more resistant to erosion than a bed of pure sand (Mitchener *et al.*, 1996).

The temperature records at M19 (Fig. 5) show that the water at this station did not become isothermal until mid-December, and both the temperature and the current meter records show the presence of near-inertial oscillations until late November. Current speeds are relatively uniform from top to bottom, with peak current speeds considerably lower than those further inshore. Near-bottom current speeds of over 0·2 m s^{-1} were observed on only four occasions: on 6 November, 2 December, 21 January and 6 February. This velocity produces a calculated bottom stress of 0·06 N m^{-2}, but no resuspension was observed. As the bottom sediment at this station is similar to that at M27, the lack of resuspension suggests that the near-bottom (5 mab) velocity required for erosion at M27 is also greater than 0·2 m s^{-1}.

At 65 mab, the temperature decreased steadily during November, but it increased sharply at 35 mab on 21 November and at the three lowest elevations on about 27 November. These changes mark the deepening of the surface mixed layer to these elevations. The vertical profile made on 5 December shows a well-developed BNL and that the water column was almost isothermal. This indicates that the breakdown of the thermocline was well advanced; the process appears to have been completed by about 10 December. Throughout the rest of the deployment, the water column remained close to isothermal and continued to cool; it first reached 4 °C (the temperature of maximum density) on January 10 and cooled to about 3 °C by the end of the deployment.

Variations in BAC at M19 are small, and all of the sensors became at least slightly fouled during the deployment. Changes in BAC at the three lowest elevations are similar until the end of December, and some of the variations also appear in the 35 and 65 mab observations. The largest increases in BAC begin on 30 November, 2 December and 5 December. As these changes do not coincide with increases in current speed, they cannot be caused by local resuspension. They do correlate with changes in temperature, so they could be the result of vertical mixing associated with the breakdown of the thermocline. However, as the BAC increases occur throughout the water column, there must also be a source for the additional material. It seems likely that the changes in BAC are caused mainly by the offshore

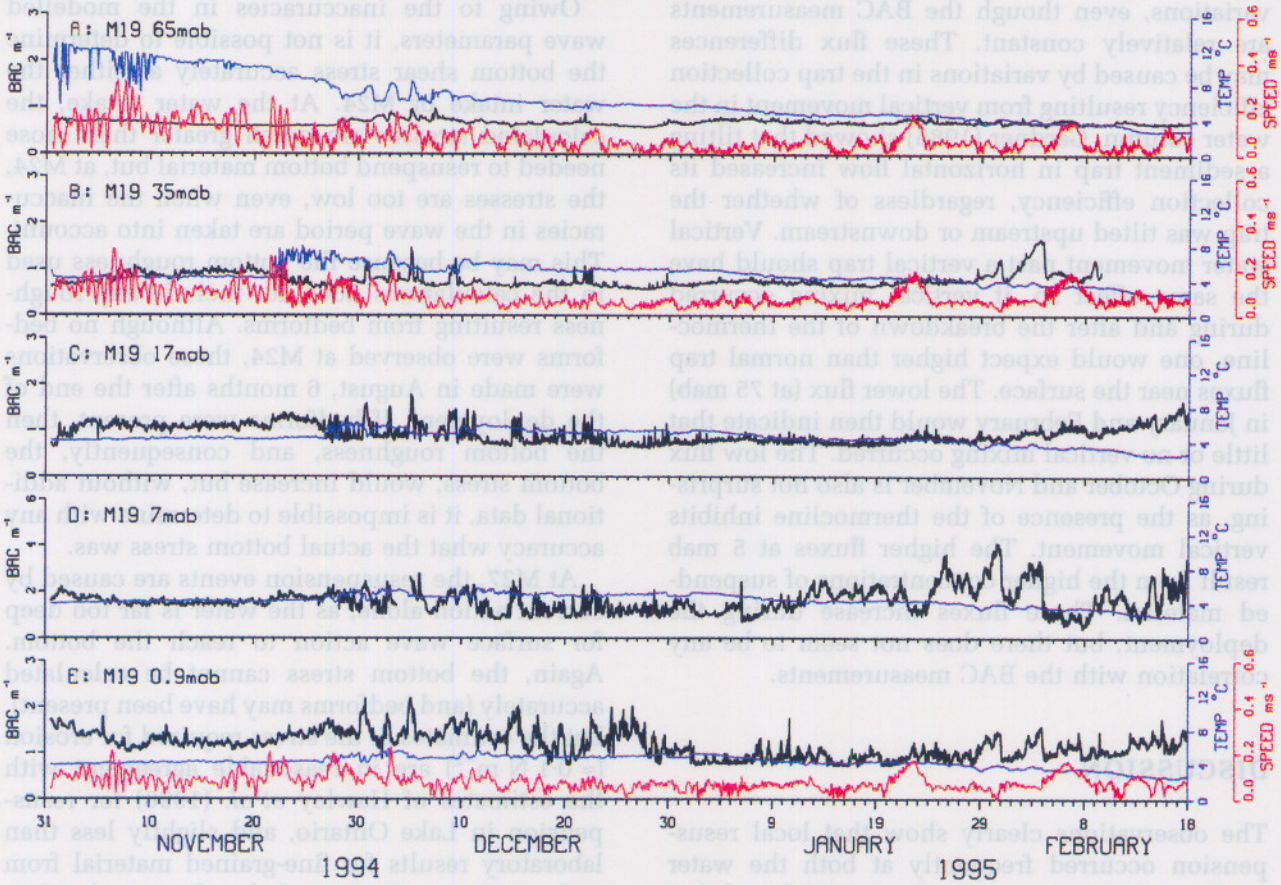

Fig. 5. Time series data from M19. Gaps in the data indicated periods when no data are available. The black line is the BAC (m^{-1}), the red line is the current speed ($m\ s^{-1}$) and the blue line is the temperature (°C). (A) Data at 65 mab (speed measured 75 mab). (B) Data at 35 mab. The LSS became severely fouled after 10 February. (C) Data at 17 mab. (D) Data at 7 mab. Note that the BAC scale is different in this plot. (E) Data at 0·9 mab (speed measured 5 mab).

advection of material resuspended further inshore. Offshore motion is observed at M27 from 26 to 29 November and at M19 from 27 November to 4 December, with a total offshore transport (at M27) of over 10 km, so material resuspended on or after November 22 could have been advected to M19. The offshore movement takes several days, however, so the material observed at M27 on and after 28 November would not have been transported this far offshore. Because of the alongshore transport that occurred, the material would have had to be resuspended from a site in a water depth of about 60 m or less, but 80–100 km further south. This would place the source of the material near the southern end of the lake, where a zone of high deposition is located (Edgington & Robbins, 1990).

Although lateral advection probably accounts for most of the variations in BAC before 5 December, vertical mixing may also be important. The increases in BAC between 15 and 25 December may also be caused by a combination of vertical mixing and lateral advection, although there is no obvious resuspension event to supply the material. The vertical profile made on 24 January shows that the 7 mab LSS was already fouled, and the other sensors appear to have become fouled shortly afterwards, so it is not possible to determine whether the resuspension event at M27 on 10 February caused an increase in BAC at M19.

One indication that vertical mixing did occur comes from the sediment traps deployed at M19 (Table 2). Monthly measurements of the mass flux 75 mab between October and February show large

Table 2. Sediment trap fluxes at M19 in g m^{-2} day^{-1}.

Dates	75 mab	3 mab
17 Oct–16 Nov	0·143	2·196
16 Nov–16 Dec	1·549	3·427
16 Dec–15 Jan	1·616	6·332
15 Jan–14 Feb	0·707	7·101

variations, even though the BAC measurements are relatively constant. These flux differences may be caused by variations in the trap collection efficiency resulting from vertical movement in the water column. Gardner (1985) showed that tilting a sediment trap in horizontal flow increased its collection efficiency, regardless of whether the trap was tilted upstream or downstream. Vertical water movement past a vertical trap should have the same effect so, if vertical mixing occurred during and after the breakdown of the thermocline, one would expect higher than normal trap fluxes near the surface. The lower flux (at 75 mab) in January and February would then indicate that little or no vertical mixing occurred. The low flux during October and November is also not surprising, as the presence of the thermocline inhibits vertical movement. The higher fluxes at 5 mab result from the higher concentrations of suspended material. These fluxes increase during the deployment, but there does not seem to be any correlation with the BAC measurements.

DISCUSSION

The observations clearly show that local resuspension occurred frequently at both the water intake and M24. Lee & Hawley (1998) found that wave action alone was sufficient to resuspend bottom material at the water intake station, and it is likely that similar events occurred during the unstratified period. The greater water depth at M24 greatly diminishes the effects of surface wave action, so the resuspension events there are probably caused by a combination of surface waves and bottom currents. Lesht & Hawley (1987) and Lee & Hawley (1998) both reported resuspension events in water depths similar to that at M24 during the stratified period. Although some of the BAC peaks in those investigations were associated with upwelling events, both investigations also found some correlation with current speed and surface wave action. Wind speeds during both investigations were only slightly less (maximum speeds of 13–14 m s^{-1}) than during this deployment, but far more resuspension events are evident in the data presented here. This may be because the absence of the thermocline allowed a more efficient transfer of wind energy from the surface of the lake to the bottom, or it may be that the conditions at the station are such that only a slight increase in wind energy is required to produce extensive bottom erosion.

Owing to the inaccuracies in the modelled wave parameters, it is not possible to determine the bottom shear stress accurately at either the water intake or M24. At the water intake, the calculated stresses are much greater than those needed to resuspend bottom material but, at M24, the stresses are too low, even when the inaccuracies in the wave period are taken into account. This may be because the bottom roughness used in the calculations does not include any roughness resulting from bedforms. Although no bedforms were observed at M24, these observations were made in August, 6 months after the end of the deployment. If bedforms were present, then the bottom roughness, and consequently, the bottom stress, would increase but, without additional data, it is impossible to determine with any accuracy what the actual bottom stress was.

At M27, the resuspension events are caused by current action alone, as the water is far too deep for surface wave action to reach the bottom. Again, the bottom stress cannot be calculated accurately (and bedforms may have been present), but the estimates of the stress required for erosion ($\approx 0{\cdot}1$ N m^{-2}) are in reasonable agreement with the estimates of Hawley *et al.* (1996) for resuspension in Lake Ontario, and slightly less than laboratory results for fine-grained material from various sites in the Great Lakes (Lee *et al.*, 1981; MacIntyre *et al.*, 1990). Estimates of the bottom stress are much better at M19. As the bottom sediment there is similar to that at M27 and as no resuspension was observed, the maximum stress observed there ($0{\cdot}06$ N m^{-2}) gives a limit for the minimum stress required for erosion at these stations.

Although Hawley *et al.* (1996) inferred resuspension events from current meter and sediment trap data, the present observations are the first direct observations of resuspension events in the Great Lakes at depths below wave base (30 m). As the storms that produced these episodes are not particularly severe, it is likely that such episodes occur fairly frequently (several times a year) during most winters. This is in marked contrast to observations during the stratified period, when no resuspension below wave base has been observed (Hawley & Lesht, 1995; Hawley & Murthy, 1995; Lee & Hawley, 1998). No resuspension was observed at M19, so bottom resuspension must be a rare occurrence (less than once a year) at this depth (101 m), but several instances of increased BAC did occur. These events were probably caused by a combination of advection and vertical mixing. The most pronounced

instances occurred during and shortly after the breakdown of the thermocline, and other episodes may have occurred later in the deployment. The occurrence of these transport episodes is consistent with the presence of the topographic waves described by Saylor *et al.* (1980).

These episodes can also explain the results of Robbins and Eadie (1991), who found that fine-grained material at a station near M19 (100 m water depth) was well-mixed throughout the water column during the non-stratified period. Robbins and Eadie (1991) explained their findings (which are based on the vertical distribution of the mass flux and of the ^{137}Cs content of trap material collected between mid-December 1982 and mid-March 1983) as resulting from the resuspension of a 'resuspendable pool' of material that they defined as a 'reservoir of particulate material contained in the benthic nepheloid region extending from a thin layer of sediments at the sediment–water interface to roughly 20 m above it' (Robbins & Eadie, 1991, p. 17084). As Robbins and Eadie had only single trap samples for the period between mid-December 1982 and mid-March 1983, they were unable to determine whether there were temporal variations in either the mass flux or the ^{137}Cs content.

Robbins and Eadie (1991) did not measure the ^{137}Cs content of the sediment in suspension, but previous studies have shown that Cs is attached primarily to fine-grained material (less than 0·60 mm), and that it is concentrated in bottom sediments located in offshore areas and in the south-eastern part of the lake (Edgington & Robbins, 1990). Fine-grained material is uncommon in the shallower parts of the lake (less than 30 m; Cahill, 1981) and, although bottom sediments in shallow water are resuspended frequently, they are rarely transported directly to the deeper parts of the lake (depths of 100 m or more). This may be because the cross-shore transport induced by the rotating two-gyre circulation is usually inhibited in shallow water by frictional effects. It is more likely that the resuspended material is first deposited at intermediate water depths (30–60 m). Although bottom material in intermediate water depths is resuspended less frequently than that in shallower water, once it is resuspended it is more likely to be transported offshore to the deeper parts of the lake. Thus, the offshore transport of material occurs as a series of hops, during each of which material is transported a small distance offshore and a far greater distance alongshore (as the currents are oriented primarily alongshore). As the currents along the east coast of the lake are primarily south to north and as the zone of maximum ^{137}Cs accumulation is centred around an area 52 m deep in the south-eastern part of the lake, material could be resuspended there and then transported to M19. Thus, alongshore advection of material resuspended about 100 km to the south may be a significant component of the material collected by Robbins and Eadie (1991). If resuspension and transport of material from the high ^{137}Cs zone does occur, then this site must act as an erosional area at least some of the time, even though over longer time spans (10–20 years) it is a depositional area.

CONCLUSIONS

The observations presented here show that, during the unstratified period, local bottom resuspension occurs fairly frequently at depths less than wave base (≈ 30 m) as a result of wave and current action, but that this material is not transported directly into the deeper parts of the lake. Instead, it is first deposited at intermediate (30–60 m) depths. Bottom resuspension at these depths by current action occurs less frequently, but material resuspended in this region is more likely to be transported offshore into the deeper parts of the lake by the ambient lake circulation. Because of the strong alongshore component of the currents, this material is also likely to be transported tens or even hundreds of kilometres alongshore, so bottom material from a single site could be redistributed throughout the lake. The observations do not support the hypothesis advanced by previous investigators that local resuspension at depths of 100 m or more is responsible for the relatively uniform sediment fluxes observed throughout the water column in the deeper parts of the lake. Rather, it appears that material transported offshore in suspension is distributed throughout the water column by vertical mixing.

The physical processes involved in sediment resuspension and transport during the unstratified period are somewhat different from those during the stratified period. Because wind speeds are generally lower during the summer, resuspension by surface wave action is less common and is restricted to shallow water. There is little evidence of offshore transport of resuspended material even during relatively strong downwelling events (Hawley & Murthy, 1995, Lee & Hawley, 1998), and there is, as yet, no evidence of any transport of material across the thermocline

into the epilimnion. During the unstratified period, the absence of a thermocline and the stronger winds allow resuspension events to occur at greater depths (up to about 60 m) where fine-grained material is more common, and the absence of the thermocline allows the freer transport of this water (and the material suspended in it) to the deeper parts of the lake.

ACKNOWLEDGEMENTS

We thank the crew of the R/V *Shenehon* for assistance during the deployment and retrieval of our moorings, and the technical staff of the Great Lakes Environmental Research Laboratory for calibrating the instruments. Weather data were provided by Clyde Sweet. Thanks also go to Bob Veneklassen of the City of Muskegon Water Filtration Plant for providing the water intake data. Gerry Miller provided the current meter data and Brian Eadie the sediment trap data at M19. Dave Schwab ran the wave model for us, and Roger Flood conducted the size analysis on the sand-sized material. Conversations with Gerry Miller, Brian Eadie, Jim Saylor and John Robbins helped to refine the ideas set forth here. Reviews of an earlier version of the manuscript by Chris Sherwood and Joe DePinto, and of the present manuscript by Barry Lesht and R. W. Duck, were extremely useful. This work was supported by the Environmental Protection Agency's Lake Michigan Mass Balance Study under interagency agreement DW 131671701. This is GLERL contribution 1071.

REFERENCES

Baker, J.E., Eisenreich, S.J. and Eadie, B.J. (1991) Sediment trap fluxes and benthic recycling of organic carbon, polycyclic aromatic hydrocarbons, and polychlorobiphenyl congeners in Lake Superior. *Environ. Sci. Technol.*, **25**, 500–509.

Boyce, F.M., Donelan, M.A., Hamblin, P.F., Murthy, C.R. and Simons, T.J. (1989) Thermal structure and circulation in the Great Lakes. *Atmosphere–Ocean*, **27**, 607–642.

Cahill, R.A. (1981) *Geochemistry of Recent Lake Michigan Sediments*. Illinois State Geological Survey Circular 517, Champaign, IL.

Colman, S.M. and Foster, D.S. (1994) A sediment budget for southern Lake Michigan, source and sink models for different time intervals. *J. Great Lakes Res.*, **20**, 215–228.

Eadie, B.J. (1997) Probing particle processes in Lake Michigan using sediment traps. *Water, Air, Soil Pollution*, **99**, 133–139.

Edgington, D.V. and Robbins, R.A. (1990) Time scales of sediment focusing in large lakes as revealed by measurement of fallout ^{137}Cs. In: *Large Lakes, Ecological Structure and Function* (Ed. by M.M. Tilzer), pp. 210–233. Springer-Verlag, New York.

Gardner, W.D. (1985) The effect of tilt on sediment trap efficiency. *Deep-Sea Res.*, **32**, 349–361.

Hawley, N. and Lesht, B.M. (1995) Does local resuspension maintain the benthic boundary layer in Lake Michigan? *J. Sedim. Res.*, **A65**, 69–76.

Hawley, N. and Murthy, C.R. (1995) The response of the benthic nepheloid layer to a downwelling event. *J. Great Lakes Res.*, **21**, 641–651.

Hawley, N. and Zyren, J.E. (1990) Transparency calibration for Lake St. Clair and Lake Michigan. *J. Great Lakes Res.*, **16**, 113–120.

Hawley, N., Wang, X., Brownawell, B. and Flood, R. (1996) Resuspension of bottom sediments in Lake Ontario during the unstratified period. 1992–93. *J. Great Lakes Res.*, **22**, 707–721.

Kim, S.-C., Wright, L.D. and Kim, B.-O. (1997) The combined effects of synoptic-scale and local-scale meteorological events on bed stress and sediment transport on the inner shelf of the Middle Atlantic Bight. *Continental Shelf Res.*, **17**, 407–433.

Lavelle, J.W., Mofjeld, M.O. and Baker, E.T. (1984) An in-situ erosion rate for a fine-grained marine sediment. *J. Geophys. Res.*, **89**, 6543–6552.

Lee, C.-H. and Hawley, N. (1998) The response of suspended particulate material to upwelling and downwelling events in southern Lake Michigan. *J. Sedim. Res.*, **68**, 819–831.

Lee, D.-Y., Lick, W. and Kang, S.W. (1981) The entrainment and deposition of fine-grained sediments in Lake Erie. *J. Great Lakes Res.*, **7**, 224–233.

Lesht, B.M. and Hawley, N. (1987) Near-bottom currents and suspended sediment concentration in southeastern Lake Michigan. *J. Great Lakes Res.*, **13**, 375–386.

MacIntyre, S., Lick, W. and Tsai, C.H. (1990) Variability of entrainment of cohesive sediment in fresh water. *Biogeochemistry*, **9**, 187–209.

Miller, M.C., McCave, I.N. and Komar, P.D. (1977) Threshold of sediment motion under unidirectional currents, *Sedimentology*, **24**, 507–527.

Mitchener, H., Torfs, H. and Whitehouse, R. (1996) Erosion of mud/sand mixtures. *Coastal Eng.*, **29**, 1–25.

Oliver, B.G. and Charlton, M.N. (1984) Chlorinated organic contaminants on settling particulates in the Niagara River vicinity. *Environ. Sci. Technol.*, **18**, 903–908.

Oliver, B.G., Charlton, M.N. and Dunham, R.W. (1989) Distribution, redistribution, and geochronology of polychlorinated biphenyl congeners and other chlorinated hydrocarbons in Lake Ontario sediments. *Environ. Sci. Technol.*, **34**, 200–208.

Rea, D.K., Owen, R.M. and Meyers, P.A. (1981) Sedimentary processes in the Great Lakes. *Rev. Geophys. Space Phys.*, **19**, 635–648.

Robbins, J.A. and Eadie, B.J. (1991) Seasonal cycling of trace elements, ^{137}Cs, ^{7}Be, and $^{239+240}$Pu in the Great Lakes. *J. Geophys. Res.*, **96**, 17081–17104.

Saylor, J.H. and Miller, G.S. (1988) Observations of Ekman veering at the bottom of Lake Michigan. *J. Great Lakes Res.*, **14**, 94–100.

Saylor, J.H., Huang, J.C.K. and Reid, R.O. (1980) Vortex modes in southern Lake Michigan. *J. Phys. Oceanogr.*, **10**, 1814–1823.

Schwab, D.J., Bennett, J.R. and Liu, P.C. (1981) Application of a simple numerical wave prediction model to Lake Erie. *J. Geophys. Res.*, **89**, 3586–3592.

Transport Canada. (1991) *Wind and Wave Climate Atlas III*. The Great Lakes Transportation Development Center, Policy and Coordination Group, Transport Canada, Ottawa, Ontario.

Manuscript received 29 June 1998;
revision accepted 11 January 1999.

© 1999 International Association of Sedimentologists, *Sedimentology*, **46**, 791–805